

***In Vivo* NMR Diffusion Spectroscopy: ^{31}P Application to Phosphorus Metabolites in Muscle**

CHRIT T. W. MOONEN,^{*,†} PETER C. M. VAN ZIJL,[‡] DENIS LE BIHAN,[§]
AND DARYL DESPRES^{*}

**In vivo NMR Research Center, BEIB, DRS, ‡Medicine Branch, NCI, and §Diagnostic Radiology Department, National Institutes of Health, Bethesda, Maryland 20892*

Received February 8, 1989; revised May 1, 1989

Apparent diffusion coefficients (D^a) of individual metabolites can be studied *in vivo* by diffusion NMR spectroscopy using an echo sequence sensitized to molecular motion. The methods are based on the echo attenuation due to phase dispersion resulting from incoherent displacement during the diffusion time. As the displacement of metabolites by diffusion *in vivo* can be affected by compartment size, temperature, adsorption processes, etc., the presented methods are potentially useful in studying such phenomena *in vivo*. Here, the methods are applied to phosphocreatine in the rat quadriceps muscle. It is demonstrated that the displacement of phosphocreatine resembles free diffusion for short diffusion times but becomes limited as a result of boundaries due to compartmentation for longer diffusion times. The limit of the displacement indicates an apparent average size of 44 μm of the compartment in the direction of the diffusion gradient. As the gradient was applied approximately parallel (angle $< 25^\circ$) to the muscle fiber, this result indicates that phosphocreatine moves freely in the cytosol but is limited by the boundaries of the muscle cells. Error analyses are performed with regard to motion artifacts and gradient performance. The methods were tested extensively for distilled water and free metabolites. © 1990 Academic Press, Inc.

INTRODUCTION

From the early days of NMR it was realized that the intensity of spin echoes (primary, secondary, as well as stimulated) is influenced by diffusion effects (1). In fact, early T_2 measurements using a single spin echo were hampered by the field gradients over the sample (2). It was also realized that the self-diffusion of molecules could be measured using a spin-echo sequence in the presence of a continuous field gradient (2). This so-called diffusion spectroscopy can be defined as echo spectroscopy sensitized to molecular motion using field gradients whose effects cancel for immobile spins but lead to incoherent phase shifts (and thus echo attenuation) for diffusing spins. The technique improved with the use of pulsed field gradients (3) so that low diffusion coefficients were obtained with better accuracy. The advent of Fourier-

† To whom correspondence should be addressed at In vivo NMR Research Center, Bldg. 10, Rm. B1D-123, National Institutes of Health, Bethesda, MD 20892.

transform techniques made it possible to study simultaneously the diffusion of different molecules in solution (4).

The echo attenuation in diffusion spectroscopy is directly related to the root-mean-square displacement of the molecule under study. Whereas *in vitro* this displacement depends on Brownian motion (in the absence of flow), the situation *in vivo* is more complicated. Apart from the pure diffusion effects, many factors may influence the displacement, e.g., local flow, boundaries of compartments which limit displacements, immobilization due to adsorption processes, transport processes, etc. Therefore, *in vivo* diffusion studies may contribute to the basic understanding of these phenomena. Similar principles as described in this paper have been applied recently to NMR imaging (5-8) and ^{31}P and ^1H NMR spectroscopy of excised tissue (9-13). Here, the first *in vivo* diffusion spectroscopy measurements are reported for phosphocreatine in rat leg muscle. Effects of compartmentation are demonstrated and analyzed. The accuracy of the methods will be discussed, in particular with respect to motion artifacts and gradient performance.

THEORY

The conventional primary spin-echo and stimulated spin-echo experiments can be easily modified for diffusion spectroscopy (Sequences 1a and 1b in Fig. 1). Ga1 and Ga2 are the "diffusion gradients" (see below). These gradient pulses also serve to disperse transverse magnetization originating from the last rf pulse in both sequences. Sequence 1a was proposed by Stejskal and Tanner (3). The diffusion Experiment 1b (14) is particularly interesting as the spins relax only with their characteristic relaxation time T_1 during the time TM. This aspect makes Sequence 1b very useful for *in vivo* studies, where T_2 is often much shorter than T_1 . Thus, the latter sequence permits the use of relatively long diffusion times without giving up large signal losses due to transverse relaxation processes (14). The small gradient pulse Gb in the TM period is not a diffusion gradient but is used to disperse any other (nonstimulated) echo that could be formed in a sequence of three rf pulses. It should be noted that gradient Gb has no effect on the diffusion measurement as the spins of interest are not in the transverse plane at the time of Gb. In addition, Gb is generally applied orthogonally to the diffusion gradients. Two additional aspects of Experiment 1b should be considered here. First, the spins eventually leading to the stimulated echo will be aligned along the z-axis by the second rf pulse. This magnetization is half of the total magnetization, only if complete dephasing has occurred during the first TE/2 period. In order to compare equal starting spin populations for the diffusion experiments, proper dephasing should be ensured even at the lowest gradient (Ga1 and Ga2) intensities. Second, in spectroscopic studies of coupled spins multiple quantum transitions are possible with a stimulated echo sequence. Contrary to transverse magnetization and higher order multiple quantum coherences, the zero-quantum contributions will not be dispersed by gradient Gb. The contribution of these effects on the final echo intensity should be analyzed on the basis of the spin systems and coupling constants.

The diffusion gradients Ga1 and Ga2 (Fig. 1) are varied in the diffusion measurements. For a spin at position I_1 at time t_1 , the effect of the square pulse Ga1 is a phase

change $\phi(I_1) = \gamma G I_1 \delta$, where G is the strength of Ga1, δ its duration, and γ is the gyromagnetic ratio. The phase is reversed by the π pulse in Experiment 1a (as well as by the combination of the two last $\pi/2$ pulses in Experiment 1b). Ga2 ($=G$) will result in a phase change $\phi(I_2) = \gamma G I_2 \delta$ at time t_2 . Thus, for immobile spins ($I_1 = I_2$) the effects of Ga1 and Ga2 cancel and the echo is attenuated only by relaxation processes. For moving spins the effects of the gradient pair no longer cancel ($I_1 \neq I_2$) and a phase change will occur. For an ensemble of incoherently moving spins (e.g., diffusion) this will cause a phase dispersion. The resulting echo attenuation has been described by Stejskal and Tanner (3) in the case of pure diffusion.

$$\frac{S}{S_0} = e^{-\gamma^2 G_1^2 \delta^2 (\Delta - \delta/3) D_1} \quad [1]$$

Here, S is the signal intensity in the presence of the gradients and S_0 is the signal intensity without the gradients (but including the relaxation effects). G_1 is the gradient strength in the I direction ($=\text{Ga1} = \text{Ga2}$). D_1 is the component of the diffusion coefficient in the I direction. Δ is the time between the start of the two gradient pulses. The root-mean-square displacement

$$\sqrt{I^2}$$

of the spins in the I direction may be expressed as

$$\sqrt{I^2} = \sqrt{2 D_1 t_{\text{dif}}}, \quad [2]$$

where t_{dif} is the diffusion time. For Experiments 1a and 1b of Fig. 1 the diffusion time is $(\Delta - \delta/3)$. To measure D_1 the gradient strength G_1 was varied (at least six different values were chosen) at constant diffusion time and the resulting echo attenuation measured. Then, $\ln(S/S_0)$ was fitted against G_1^2 according to Eq. [1] (cf. Figs. 2 and 3). The term "displacement" will refer to root-mean-square displacement throughout this paper.

MATERIALS AND METHODS

The studies were performed with a 4.7-T GE CSI NMR instrument equipped with a prototype of self-shielded gradients with gradient strength up to 2 G/mm on each axis. Temperature was adjusted using a chamber surrounded by a water blanket. The temperature was measured at four places close to the sample using a fluoroptic thermometer (Luxtron). For *in vivo* measurements the rectal temperature of the rat was measured as well as the skin temperature at three places close to the region of interest (accuracy $\pm 1^\circ\text{C}$). Rectal temperature was kept constant at 37°C . Rectal and skin temperatures were identical to within 2°C .

The experiments were performed using home-made solenoid coils tuned to the ^{31}P or ^1H NMR frequency. Radius and width of the ^1H rf coil were 8 and 10 mm, respectively. A plastic sphere ($r_i = 3$ mm) filled with distilled water was placed in the center for ^1H NMR measurements. Radius and width of the ^{31}P rf coil were both 12 mm. For the *in vitro* experiments a plastic sphere ($r_i = 8$ mm) was placed in the center of the solenoid. A solution was prepared containing 20 mM adenosine triphosphate (ATP), 20 mM phosphocreatine (PCr), 20 mM phosphate (P_i), and 20 mM phos-

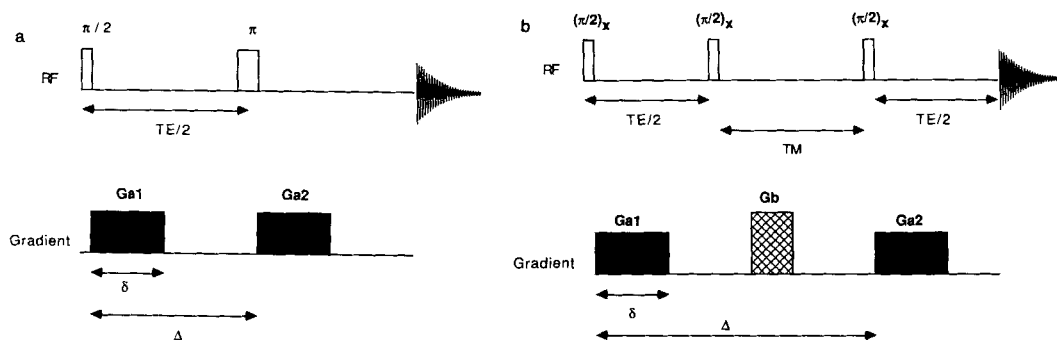


FIG. 1. Pulse sequences for diffusion spectroscopy. Sequence (a) is the primary spin echo. Sequence (b) is the stimulated spin echo. Acquisition period starts on top of the echo. Ga1 and Ga2 are the "diffusion gradients" (see text). Gb serves to disperse all other echoes formed in this sequence. δ is the duration of the diffusion gradient. Δ is the time between the start of the two diffusion gradients.

phoethanolamine (PE) in distilled water (pH 7.0). For *in vivo* experiments the left hind leg of a Sprague-Dawley rat was inserted in the ^{31}P rf coil. The leg was positioned with gauze. The rat was stabilized against a plastic holder. This experimental setup was chosen to avoid any variation in coil loading and rf inhomogeneity during cardiac or respiratory cycle. Anesthesia was achieved using isoflurane (1%) and a nitrous oxide to oxygen ratio of 7/3. Shimming was performed by maximizing the integrated ^{31}P signal in an echo experiment. ^{31}P linewidths in phantom and rat quadriceps muscle were about 3 and 20 Hz, respectively.

RESULTS AND DISCUSSION

In Vitro Experiments

Sequences 1a and 1b (Fig. 1) were used for a series of tests on accuracy and reproducibility of diffusion spectroscopy measurements using different gradient duration times δ and diffusion times $(\Delta - \delta/3)$. The results for distilled water at 21°C are similar using Sequence 1a or 1b. The data obtained with the primary echo are summarized in Table 1. It can be seen that all values compare favorably with the literature value of $2.09 \times 10^{-3} \text{ mm}^2 \text{ s}^{-1}$ at this temperature (interpolated from data of Ref. (15)). This indicates that the experimental NMR setup allows accurate determinations of diffusion constants over a wide range of diffusion time and gradient durations. The accuracy and possible artifacts will be discussed below.

^{31}P diffusion NMR spectroscopy was applied to determine the diffusion constants of some metabolites *in vitro*. Figure 2a shows a stacked plot of progressive attenuation due to diffusion as a function of the diffusion gradient strength using Sequence 1b on a phantom containing phosphorylated compounds usually present in *in vivo* ^{31}P NMR spectra (see Material and Methods). The resonance linewidths are independent of the amplitude of the diffusion gradients indicating negligible residual gradient effects during the acquisition time. Figure 2b shows a plot of $\ln(S/S_0)$ as a function of the square of the gradient strength together with the computed linefit according to Eq. [1]. The regression coefficient p was >0.995 for all resonances. For reasons of

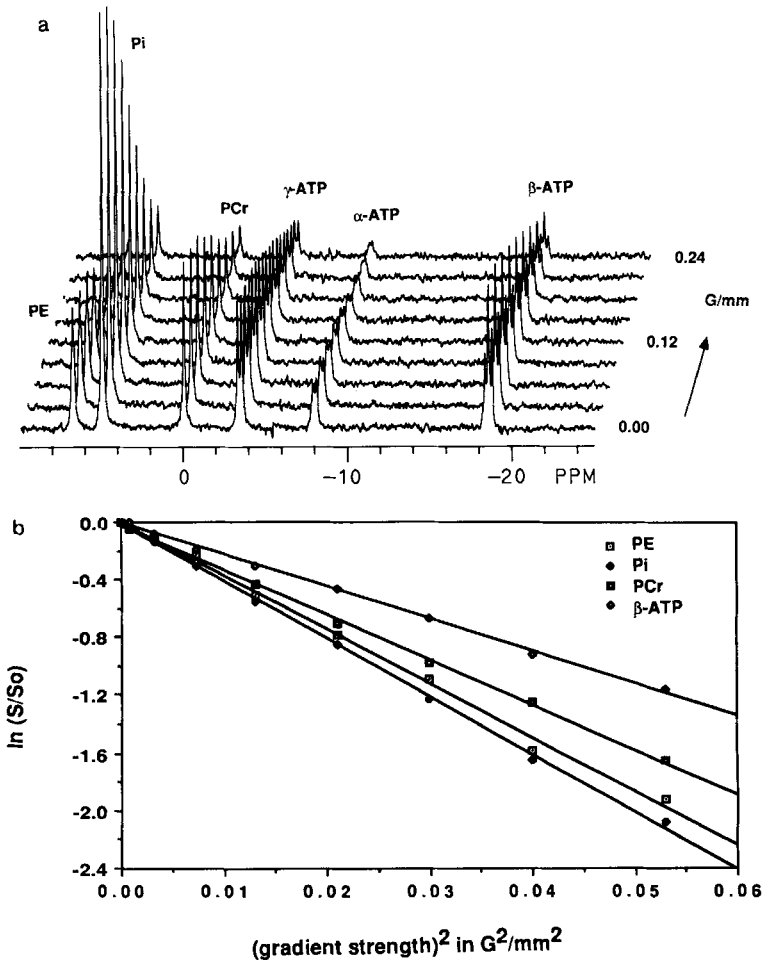


FIG. 2. (a) Progressive attenuation of ^{31}P stimulated echo intensity upon increasing gradient strength in a phantom sample at 37°C ; $\text{TE} = 100$ ms and $\text{TM} = 500$ ms. The strength of the diffusion gradients (G_1 and G_2) was increased in steps of 0.03 G/mm. The TM gradient (G_b) was 0.2 G/mm during 4 ms. Resonances are marked as follows: PE, phosphoethanolamine; P_i , inorganic phosphate; PCr, phosphocreatine; γ -ATP, α -ATP, and β -ATP, γ , α , and β phosphate of adenosinetriphosphate. Note that no echo signal losses due to multiple quantum transitions occur at $\text{TE} = 100$ ms (i.e., the second rf pulse occurs at $J^{-1} = 50$ ms). (b) Natural logarithm of the ratio S/S_0 versus square of gradient strength. The drawn lines are the computed line fits according to Eq. [1] (regression coefficient > 0.995 for all resonances). The three resonances of ATP all lead to a similar diffusion coefficient (cf. Table 2), but only the β -ATP resonance is included in the figure for the sake of clarity.

clarity the values of only one ATP resonance are shown in Fig. 2b. The diffusion coefficients are summarized in Table 2. As can be expected the calculation of the diffusion coefficient of ATP using either γ , α , or β phosphate resonance yields similar results.

For the *in vitro* measurements the diffusion coefficient should be independent of the diffusion time as no physical boundaries for a restricted diffusion exist. This is

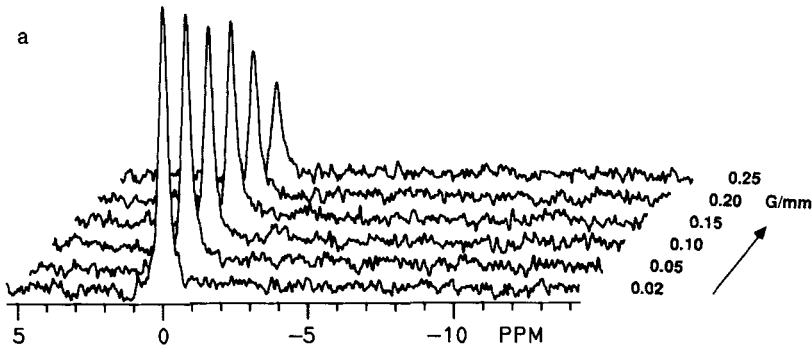


FIG. 3a. Progressive attenuation of ^{31}P stimulated echo intensity upon increasing gradient strength for phosphocreatine in the rat quadriceps muscle; TE = 100 ms and TM = 500 ms. All resonances except phosphocreatine are decreased beyond detection due to T_2 losses. The strength of the diffusion gradients (Ga1 and Ga2) was increased as indicated on the right of the spectra. The TM gradient (Gb) was 0.2 G/mm during 4 ms. No appreciable line broadening due to residual gradient effects occurred since fitting of the phosphocreatine lineshape resulted in the following linewidths at half height: 20.3, 20.6, 20.1, 20.2, 20.8, and 20.7 Hz for the six spectra shown.

indeed found for water (Table 1) as well as all phosphorylated compounds (Table 2). It can be seen that the diffusion constants of the different phosphorylated compounds show a correlation with molecular weight. However, it is interesting to note that the relatively large molecule as ATP has a diffusion coefficient more than half that of inorganic phosphate. Apparently, the effective size of the hydrated molecules is rather similar at the ionic strength used. From Table 2 it is evident that the temperature has a drastic influence on the diffusion coefficient. At 37°C the diffusion coefficient of all phosphorylated compounds becomes about 50% larger. This increase correlates well with the increase in diffusion of pure water over this temperature change (10, 16).

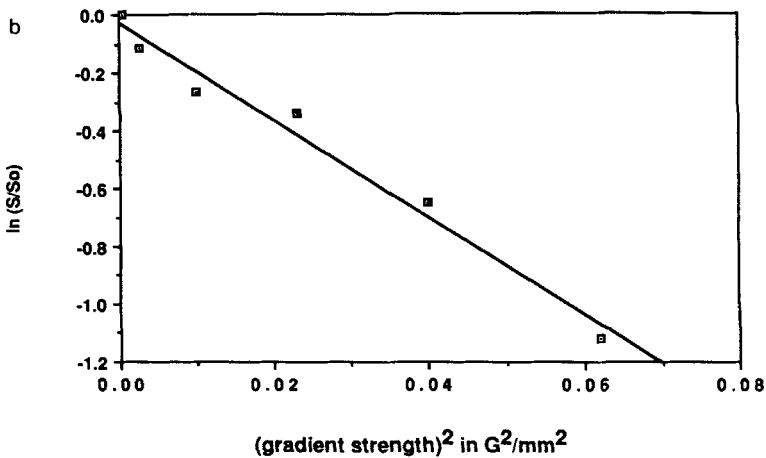


FIG. 3b. Natural logarithm of the ratio S/S_0 versus square of gradient strength. The drawn line is the computed line fit according to Eq. [1] (regression coefficient = 0.99).

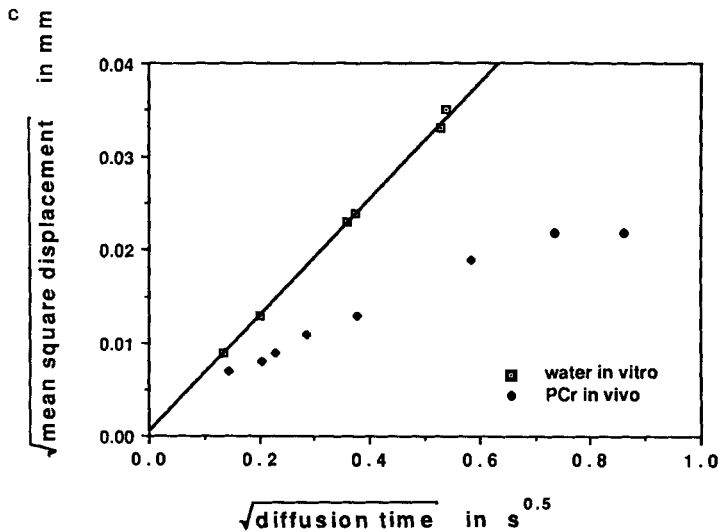


FIG. 3c. Root-mean-square displacement of phosphocreatine *in vivo* as a function of the square root of the diffusion time. If the displacement is due to unrestricted diffusion (no boundaries), the points should follow a straight line through zero (cf. Eq. [2]). This is indicated for pure water (see data Table 1). The drawn line is the computed line fit of the data to Eq. [2].

In Vivo Experiments

Figure 3a shows the results of an *in vivo* diffusion experiment on the hind leg of a Sprague–Dawley rat. A stimulated echo sequence with TE of 100 ms and TM of 500 ms was used for this experiment. The rather long TE time resulted in large T_2 losses for all compounds except phosphocreatine. We will therefore concentrate on the analysis of the diffusion of this compound *in vivo*. Figure 3b shows a plot of $\ln(S/S_0)$ versus the square of the gradient strength indicating a satisfactory fit according to Eq. [1]. It should be noted that one cannot assign a pure diffusion coefficient as

TABLE 1
Diffusion Coefficient of Distilled Water at 21°C as a Function
of the Diffusion Time ($\Delta - \delta/3$)

Diffusion time t_{diff} (ms)	Gradient duration δ (ms)	Diffusion constant ^a D ($10^{-3} \text{ mm}^2 \text{ s}^{-1}$)
19	19	2.14
42	25	2.12
142	25	2.04
130	61	2.08
280	61	1.96
292	25	2.05

^a As determined with Sequence 1a of Fig. 1. TE equals 2Δ in all experiments. Estimated accuracy of the diffusion coefficient is within 5%.

TABLE 2

Diffusion Coefficient of Phosphorylated Metabolites at 23 and 37°C as a Function of the Diffusion Time, Gradient Duration, and ^{31}P Diffusion NMR Method Used

Resonance	Diffusion constant D (in $10^{-3} \text{ mm}^2 \text{ s}^{-1}$)				
	At 37°C			At 23°C	
	Expt. 1	Expt. 2	Expt. 3	Expt. a	Expt. b
PE	0.93	0.94	0.93	0.56	0.60
P_i	1.02	1.00	1.06	0.70	0.70
PCr	0.81	0.78	0.84	0.50	0.54
γ -ATP	0.58	0.60	0.58	0.39	0.39
α -ATP	0.56	0.60	0.62	0.39	0.35
β -ATP	0.56	0.56	0.52	0.40	0.39

Note. See Material and Methods for details of sample composition. The following sequence, diffusion time, and gradient duration were used: Experiment 1, stimulated echo, 142 ms, 25 ms; Experiment 2, stimulated echo, 542 ms, 25 ms; Experiment 3, primary echo, 120 ms, 60 ms; Experiment a, stimulated echo, 96 ms, 11 ms; Experiment b, primary echo, 130 ms, 60 ms.

the sole basis of the effective mean-square displacement of phosphocreatine *in vivo*. The effective displacement may be the result of binding to macromolecules or microcirculation inside the cell. Microcompartmentation may impose local boundaries to the effective displacement. Therefore, we will call this *in vivo* diffusion coefficient as measured with NMR spectroscopy the apparent diffusion coefficient (D^a) following the convention proposed for imaging of intravoxel incoherent motion (5). The results are summarized in Table 3. For short diffusion times the D^a of phosphocreatine *in vivo* is similar to the *in vitro* diffusion coefficient indicating that, for short diffusion

TABLE 3

Apparent Diffusion Constant (D^a) of Phosphocreatine in the Rat Quadriceps Muscle as a Function of the Diffusion Time and Gradient Duration

Diffusion time t_{dir} (ms)	Gradient duration δ (ms)	D^a ($10^{-3} \text{ mm}^2 \text{ s}^{-1}$)
21	13	1.23 ^p
42	25	0.73 ^p
52	25	0.80 ^s
82	25	0.73 ^s
142	25	0.60 ^s
342	25	0.53 ^s
542	25	0.43 ^s
742	25	0.33 ^s

Note. Apparent diffusion coefficients marked with p and s were obtained with the primary echo and stimulated echo, respectively.

times, the majority of phosphocreatine is freely moving in a microviscosity resembling the macroscopic viscosity of pure water.

The relation of displacement and diffusion time is interesting because it may show a transition from free toward restricted motion at a diffusion time corresponding with a displacement approaching the compartment size (17–19). The effects of such compartmentation can be clearly seen in the displacement of phosphocreatine *in vivo* (Fig. 3c) and in the D^a values (Table 3). If no boundaries exist the displacement is proportional to the square root of the diffusion time. The results for pure water are added to Fig. 3c to demonstrate the straight line through zero according to Eq. [2]. For short diffusion times the displacement of phosphocreatine *in vivo* is independent of the boundaries as the displacement is still much less than the compartment size. From Fig. 3c it can be seen that the displacement is indeed linearly dependent on the square root of the diffusion time until the displacement reaches a limit of 20–22 μm indicating the effects of restricted motion. The average mean-square displacement in a particular direction is half the size of the compartment in that direction assuming equal spatial distribution of molecules in this compartment. Thus, the apparent compartment size is about 44 μm in the direction of the gradient, which was approximately ($<25^\circ$ angle) parallel to the hind leg. This size correlates well with the length of the muscle cells. All these results indicate that the majority of phosphocreatine moves freely in the cytosol but is limited by the boundaries of the muscle cells.

It should be noted that the calculated displacement should be used only as a first approximation of the actual compartment size, because the calculations of the mean-square displacements (using Eq. [2]) are based on a Gaussian distribution of metabolite displacement upon time (Brownian diffusion). In the case of restricted diffusion deviations from the Gaussian distribution occur near the boundaries. As the actual distribution (and thus the calculated size of the compartment) depends on the shape of the compartment (19) the calculated size is only an “apparent compartment size.” The actual size can be better approached when the geometry of the restricted volume is well defined (19).

Another problem arises when molecules can “escape” from the restricted volume according to permeability effects (11). This is especially true for water molecules. The study of pure intracellular metabolites such as phosphocreatine eliminates this source of error.

Artifacts in in Vivo Diffusion Spectroscopy

(1) *Motion artifacts.* Sequences 1a and 1b are “sensitized” to molecular displacement and are therefore in principle sensitive to any motion. This is potentially a serious problem as we are dealing with at least the motions due to the cardiac and respiratory cycle, in addition to possible vibrations of the gradients translating to the sample. Moreover, because the calculations of the diffusion constants are based on displacements of less than 20 μm (see above) it is important to address these potential problems carefully.

In this respect it is important to distinguish incoherent from coherent effects. Diffusion results in an incoherent displacement, giving rise to a phase dispersion of the spins, and finally to an echo attenuation. In contrast, any overall motion such

as cardiac and respiratory motion or vibrations originating from the gradient coils generally results in a coherent displacement of mass in the region of interest leading to an overall phase change rather than a phase dispersion. The overall phase change can be easily corrected. However, if subsequent scans are added asynchronous with the motion, the changing phase due to the coherent motion leads to an apparent echo attenuation after several scans (temporal incoherence). For phosphocreatine *in vivo* this can be easily tested as the S/N was at least 10 in a single scan using diffusion spectroscopy. The phase change in single scan experiments was monitored upon increasing diffusion gradients G_{a1} and G_{a2} for different diffusion times and gradient durations without any gating. No phase changes could be observed within the accuracy of the experiments. Moreover, the D^a on the basis of single-scan experiments was similar to the D^a on the basis of multiple-scan experiments. This indicates that the region of interest did not experience any coherent displacements of more than a few micrometers. In addition, the motions resulting from cardiac and respiratory cycle are expected to cause displacements and dephasings which increase upon increasing diffusion times (the diffusion times used in this study are generally smaller than the respiratory or cardiac cycle). In contrast, the *in vivo* results show a decrease of D^a even after relatively short diffusion times. Thus, we conclude that the *in vivo* diffusion measurements reported here were not influenced by macroscopic motions, although small amplitude (a few micrometers) coherent motions cannot be excluded.

The *in vitro* studies show diffusion constants independent of the diffusion time. The calculated diffusion coefficient of water is in agreement with literature values based on different methods. This rules out possible errors due to mechanical vibration in the magnet/gradient system.

(2) *Gradient effects.* The experiments described here impose special specifications on the gradient system. First, the residual gradient effects during the signal acquisition have to be minimized. The following calculation may serve as an illustration. For *in vivo* experiments using a diffusion time of 21 ms and a gradient duration of 13 ms, the gradient strength leading to S/S_0 of 0.5 was about 1.4 G/mm. Since the sample diameter was about 20 mm the gradient over the sample amounted to 28 G resulting in a spread in Larmor precession frequency of about 48,000 Hz during the gradient pulses. The magnetic field should again be homogeneous during the acquisition time. In the example of phosphocreatine *in vivo* (linewidth at half height was 20–22 Hz), an additional line broadening of 10% (about 2 Hz) due to residual gradient effects may be acceptable for many applications. This means that such residual gradient effects during the acquisition time (about 0.5 s) should be less than or equal to 0.005% of the maximum strength used. This may necessitate the use of self-shielded gradients with efficient quenching of mechanical vibration and a highly stable power amplifier. In order to minimize residual gradient effects it is advantageous that the diffusion gradients are placed in the beginning of each $TE/2$ period (Fig. 1) followed by a gradient stabilization period. In addition, the linewidth of the resonances under study should be carefully monitored for all diffusion gradient strengths used. For the example given above, using a gradient duration of 13 ms and a diffusion time of 21 ms ($TE = 50$ ms), the resonance linewidth of phosphocreatine increased from 21 Hz without diffusion gradients to 22.5 Hz with 1.4 G/mm for G_{a1} and G_{a2} .

A second gradient problem is the exact equivalence of gradients G_{a1} and G_{a2} . Instabilities and residual gradient effects cause inequivalence of the two gradients and

improper refocusing. The instabilities have to be minimized. The calculations above may serve as an example for the requirements of stability. This may again necessitate shielded gradients with a highly stable power amplifier. In addition, one of the gradients should be independently adjustable for optimal refocusing. This was not necessary for the measurements reported here. It should be mentioned that the diffusion experiments described here do not impose high demands on gradient rise and fall times. One may actually consider lengthening the rise and fall time in order to minimize residual gradient effects during the acquisition time.

ACKNOWLEDGMENTS

The authors are grateful to General Electric NMR Instruments for making available the prototype set of shielded gradients built by Dr. Pete Roemer of GE Corporate R & D. In addition, we thank Scott Chesnick, Kyle Hedges, Robert Turner, David Hoult, and Jack Cohen for stimulating discussions and support. This work was performed in the NIH In Vivo NMR Research Center.

REFERENCES

1. E. L. HAHN, *Phys. Rev.* **80**, 580 (1950).
2. H. Y. CARR AND E. M. PURCELL, *Phys. Rev.* **94**, 630 (1954).
3. E. O. STEJSKAL AND J. E. TANNER, *J. Chem. Phys.* **42**, 288 (1965).
4. T. L. JAMES AND G. G. McDONALD, *J. Magn. Reson.* **11**, 58 (1973).
5. D. LE BIHAN, E. BRETON, D. LALLEMAND, P. GRENIER, E. CABANIS, AND M. LAVAL-JEANTET, *Radiology* **161**, 401 (1986).
6. D. G. TAYLOR AND M. C. BUSHELL, *Phys. Med. Biol.* **30**, 345 (1985).
7. K. MERBOLDT, W. HÄNICKE, AND J. FRAHM, *J. Magn. Reson.* **64**, 479 (1985).
8. W. SATTIN, T. H. MARECI, AND K. N. SCOTT, *J. Magn. Reson.* **65**, 298 (1985).
9. K. YOSHIZAKI, Y. SEO, H. NISHIKAWA, AND T. MORIMOTO, *Biophys. J.* **38**, 209 (1982).
10. D. C. CHANG, H. E. RORSCHACH, B. L. NICHOLS, AND C. F. HAZLEWOOD, *Ann. N.Y. Acad. Sci.* **204**, 434 (1973).
11. J. E. TANNER, *Biophys. J.* **28**, 107 (1979).
12. G. G. CLEVELAND, D. C. CHANG, C. F. HAZLEWOOD, AND H. E. RORSCHACH, *Biophys. J.* **16**, 1043 (1976).
13. H. E. RORSCHACH, D. C. CHANG, C. F. HAZLEWOOD, AND B. L. NICHOLS, *Ann. N.Y. Acad. Sci.* **204**, 444 (1973).
14. J. E. TANNER, *J. Chem. Phys.* **52**, 2523 (1970).
15. R. MILLS, *J. Phys. Chem.* **77**, 685 (1973).
16. J. H. SIMPSON AND H. Y. CARR, *Phys. Rev.* **111**, 1201 (1958).
17. J. ANDRASKO, *J. Magn. Reson.* **21**, 479 (1976).
18. R. L. COOPER, D. B. CHANG, A. C. YOUNG, C. J. MARTIN, AND B. ANKER-JOHNSON, *Biophys. J.* **14**, 161 (1974).
19. J. E. TANNER AND E. O. STEJSKAL, *J. Chem. Phys.* **49**, 1768 (1968).